EURASIP Journal on Wireless Communications and Networking
a SpringerOpen Journal

RESEARCH Open Access

Burst allocation method to enable decision-directed channel estimation for mobile WiMAX downlink transmission

Yu-Sun Liu[1*], Shingchern D You[2] and Reui-kai Wu[1]

Abstract

An easy-to-implement approach to allocate downlink data bursts in IEEE 802.16e (mobile WiMAX) frames is proposed. With the proposed allocation scheme, each mobile station can employ a decision-directed channel estimation method without demodulating data bursts destined for other stations. Three decision-directed channel estimation methods, each with different computational complexity, are suggested based on the proposed allocation method. Theoretical analysis and simulation results show that one of the suggested decision-directed methods, the adaptive weighted-average estimation, outperforms the widely used two-dimensional interpolation method for all considered channel models, especially for high-speed reception in a large-delay-spread channel. Therefore, the proposed allocation method together with the adaptive weighted-average estimation can be used to increase the successful transmission probability for data bursts requiring low error rates, such as hybrid automatic repeat request bursts.

Keywords: WiMAX, Burst allocation, Decision-directed channel estimation

1. Introduction

The mobile worldwide interoperability for microwave access (mobile WiMAX) technology, based on IEEE 802.16e [1], is a wireless metropolitan network standard and a candidate for fourth-generation cellular wireless communication systems. To serve multiple mobile stations (MSs), the mobile WiMAX adopts the orthogonal frequency division multiple access (OFDMA) technique. Since the OFDMA signal is transmitted through a wireless environment, the receivers have to perform channel estimation to compensate for channel fading before demodulation and decoding. Although both downlink (DL) and uplink (UL) transmissions of WiMAX use OFDMA, these two systems have different design considerations and different pilot patterns, and thus, they have to use different channel estimation strategies. In this paper, we investigate the channel estimation method for the WiMAX DL transmission, in which the base station (BS) transmits data destined for different MSs by using different sets of subcarriers. Therefore, instead of demodulating and decoding every subcarrier in all OFDMA symbols in the DL transmission, each MS only has to process subcarriers containing broadcast data and data destined for itself.

Many channel estimation methods have been studied in the literature for various systems [2-14]. These methods can be divided into several categories: minimized mean square error (MMSE)-based methods, filter-based methods, discrete Fourier transform (DFT)-based methods, code-aided methods, linear and cubic interpolation methods, and decision-directed methods. The MMSE-based methods make use of the statistics of the wireless channel for channel estimation and achieve excellent bit error rate (BER) performance in a low-mobility environment [2-4]. As the stochastic property of a real channel is actually unknown, Nisar et al. [5] proposed a maximally robust two-dimensional (2-D) MMSE channel estimator with a finite number of observations. However, this approach works only for a uniformly spaced pilot pattern and thus cannot be applied to the mobile WiMAX DL system due to non-uniformly spaced pilot patterns in the system. Sanzi and Speidel [6]

* Correspondence: yuliu@ntut.edu.tw
[1]Department of Electronic Engineering, National Taipei University of Technology, 1, Sec. 3, Chung-Hsiao E. Rd., Taipei 106, Taiwan
Full list of author information is available at the end of the article

proposed another channel statistic estimation method in which the Doppler frequency shift and the delay were assumed to be uniformly distributed, and receivers have to use different sets of pre-computed coefficients for different channels. However, how to determine the number of coefficient sets remains a question.

Filter-based channel estimation uses different types of filters to act as interpolation filters [3,7]. The DFT-based approach [2,3,8] performs inverse discrete Fourier transform on pilot subcarriers to find the channel impulse response and then proceeds to find the channel frequency response (CFR) with DFT. Both approaches assume a uniformly spaced pilot pattern and thus cannot be applied to the mobile WiMAX DL system. Code-aided methods [9-11] make use of the *posteriori* probabilities (obtained by the decoder) of all the transmitted symbols in one orthogonal frequency division multiplexing (OFDM) symbol for channel estimation in OFDM systems. Further investigation is required to apply these methods to the WiMAX OFDMA systems.

The 2-D linear interpolation method [12] is the most widely used estimation method in mobile WiMAX. Unfortunately, this method does not provide satisfactory BER performance for large-delay-spread channels [8]. To achieve better BER performance, a cubic interpolation function with coefficients obtained by a search algorithm was proposed for interpolation in the frequency direction in [13]. Although this method performs relatively better for a channel with a large delay spread, its BER performance is still far away from the perfect channel estimation.

The decision-directed (DD) estimation is a robust method for channel estimation [14]. In the method, contents of data subcarriers of an OFDM symbol are decoded and then encoded. Next, CFRs of these data subcarriers are re-estimated using the least squares (LS) method for better accuracy. With better estimation of CFRs of previous OFDM symbols, the CFRs of the current OFDM symbol can be more accurately estimated. Though robust, it is difficult to apply the DD method to mobile WiMAX DL transmission since the allocation of subcarriers in OFDMA symbols for data bursts destined for each MS is highly flexible. Therefore, an MS may have to demodulate and decode data addressed to other MSs in order to implement the DD method. To avoid extra demodulation and decoding cost, we propose a burst allocation scheme so that an MS only needs to demodulate and decode broadcast data and data destined for itself (which the MS has to process regardless whether the DD method is employed) if the MS intends to use the DD method to improve the accuracy of CFR estimation. Based on the proposed allocation, we further suggest three DD channel estimation methods for mobile WiMAX DL transmission.

The rest of the paper is organized as follows. Section 2 briefly reviews the frame structure, encoding flow, and pilot pattern in the mobile WiMAX DL transmission. Section 3 describes the 2-D and DD channel estimation methods. In Section 4, we propose a burst allocation scheme and suggest three DD channel estimation methods based on the allocation scheme. Theoretical analysis and experimental results of the performances of the proposed DD channel estimation methods are presented in Section 5, and finally, conclusions are drawn in Section 6.

2. Overview of WiMAX physical layer

Before we describe the proposed burst allocation scheme, we briefly review the frame structure, encoding process, and pilot pattern in the mobile WiMAX DL transmission.

2.1 WiMAX frame structure

Although the 802.16e standard supports many duplexing and physical (PHY) layer schemes for UL and DL transmissions, the mobile WiMAX system supports only time-division duplex (TDD) with wireless MAN-OFDMA PHY [15]. In the TDD scheme, frames are sequentially transmitted over time, with each frame containing a DL subframe and a UL subframe. In the DL subframes, data subcarriers in each OFDMA symbol are grouped into logical subchannels which, in turn, may be allocated to data bursts for different MSs in several ways. However, in this paper, we will only discuss the partial usage of subchannel (PUSC) allocation scheme (detailed below) as it is the mandatory allocation scheme for the first zone in each DL subframe.

As shown in Figure 1, a DL subframe consists of a preamble, frame control header (FCH), downlink map (DL-MAP), uplink map (UL-MAP), and downlink data bursts. The preamble in each DL subframe occupies one OFDMA symbol. Other than the preamble, the coded data are allocated in the unit of slot, where one slot is a spectral-temporal rectangular structure containing one logical subchannel in a pair of OFDMA symbols. Logical subchannels are numbered from top to bottom in OFDMA symbols, as also shown in Figure 1. Note that there is a permutation function that maps each logical subchannel to a group of 24 physical data subcarriers. The FCH occupies the first four slots in the first pair of OFDMA symbols after the preamble. Then, DL-MAP is allocated to the subsequent slots in the same pair of OFDMA symbols from top to bottom and, if necessary, may extend to the next pair of OFDMA symbols. DL-MAP is followed by UL-MAP (which is located in the DL burst no. 1) and DL bursts (each of which may be addressed to different MSs).

The contents of FCH specify the coding scheme and length of DL-MAP. With the information in FCH, MSs

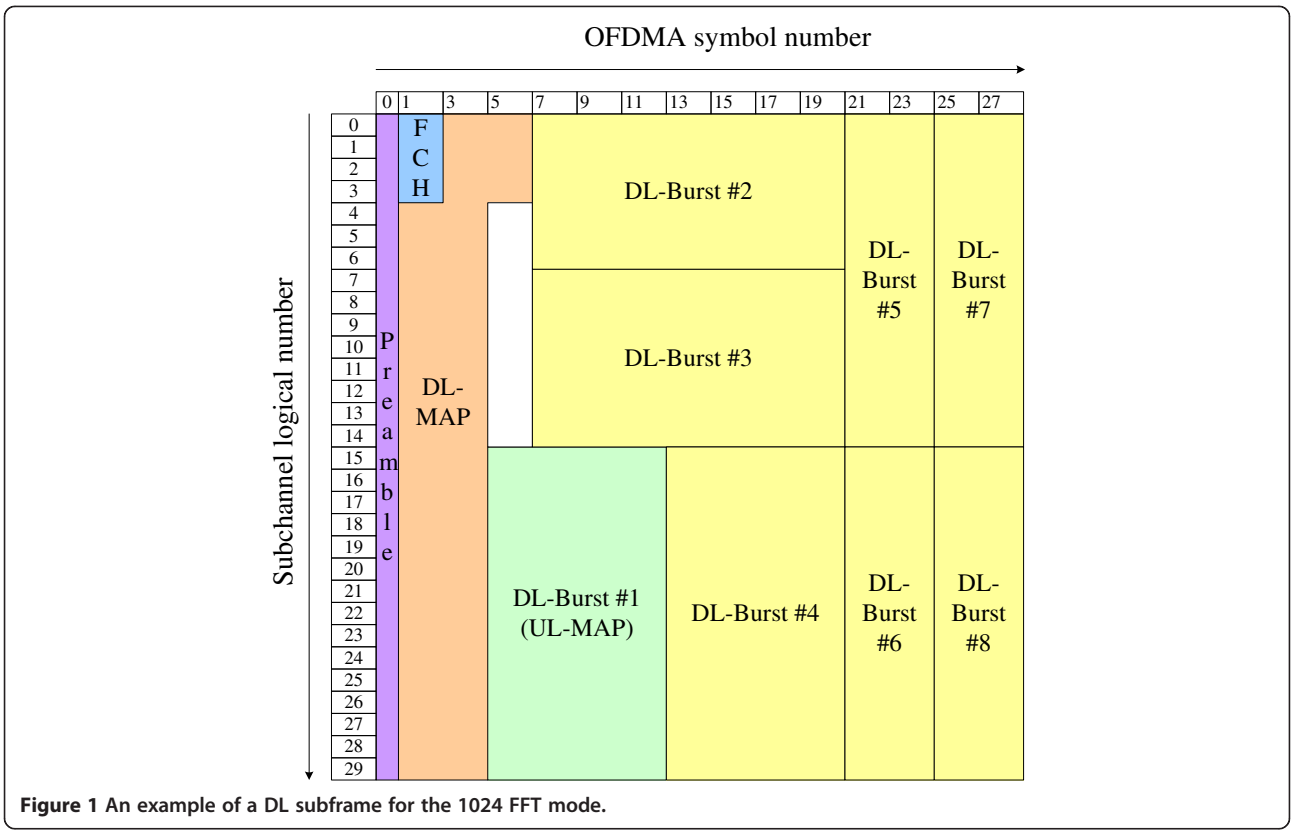

Figure 1 An example of a DL subframe for the 1024 FFT mode.

can then decode DL-MAP. In the DL-MAP, burst profiles of the DL bursts are specified, such as modulation and coding schemes, locations in the DL subframe, and destination MSs. Therefore, all MSs must correctly decode FCH and DL-MAP before proceeding to decode DL bursts. Since the 48-bit-long FCH is constructed by duplicating the 24-bit-long DL_Frame_Prefix, any error in the FCH can be easily detected by comparing the two copies of the DL_Frame_Prefix. As DL-MAP contains a CRC-32 field for error detection, it is also easy for an MS to check the correctness of DL-MAP.

The structure of each DL burst is a rectangle with one or multiple slots. Coded bits (in the unit of slot) are sequentially mapped to a DL burst in increasing order of the subchannel number in the first available pair of symbols. When all slots in the first available pair of symbols of the burst are filled, the mapping process continues to the next available pair of symbols, and so on. Typically, different DL bursts are destined for different MSs. Therefore, in order to implement the DD method, an MS may have to demodulate and decode data addressed to other MSs (to be justified in Section 3.2). In Section 4, we propose a DL burst allocation scheme which not only complies with the standard but also enables MSs to use the DD approach without incurring the cost of unnecessary demodulation and decoding.

2.2 DL encoding

The channel coding procedure in the physical layer of DL transmission includes randomization, forward error correction (FEC) encoding, interleaving, and modulation, as shown in Figure 2. Data bits are first divided into FEC blocks with padding bits, if necessary. The size of an FEC block, which is in the order of tens of bytes, is determined based on data length, code rate, and modulation scheme. Each FEC block is then separately randomized, FEC-encoded, interleaved, and modulated. The 802.16e standard supports convolutional code (CC), block turbo code, convolutional turbo code, and low-density parity-check code, but only CC is mandatory. Therefore, we use CC in the experiments. After randomization, each FEC block is encoded by the binary

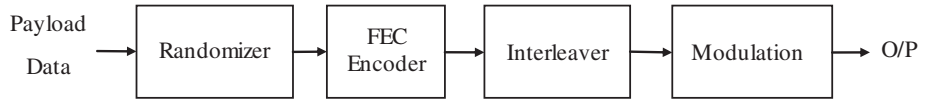

Figure 2 Encoding and modulation flow for DL data transmission.

(171, 133) convolutional encoder with a constraint length of 7. Before encoding, the encoder memory is initialized with the last six data bits of the FEC block to be encoded. Thus, the initial state of the code trellis is the same as the end state, and the convolutional code is converted into a short block code called tail-biting convolutional code (TBCC) [16,17]. Each codeword, which is called coded FEC block, is interleaved and constellation-mapped into modulation symbols that in turn are mapped to slots of the data burst. Each data burst may contain more than one coded FEC blocks. According to the standard [1], a coded FEC block occupies at most six slots.

2.3 Pilot subcarriers in the DL subframe

For each pair of OFDMA symbols, the available subcarriers are grouped into clusters. Each cluster consists of 12 data subcarriers and 2 pilot subcarriers, as shown in Figure 3, where a gray circle stands for a data subcarrier and a slashed one stands for a pilot subcarrier. In contrast to conventional OFDM systems with equally spaced pilots, such as DVB-T [18], the pilots in the WiMAX DL subframe not only are unevenly distributed but also have different distribution patterns in even and odd symbols. Therefore, it is expected that any channel estimation method based on interpolating only pilot CFRs in one OFDMA symbol is unlikely to provide good estimation accuracy, especially for large-delay -spread channels [13].

3. Channel estimation in WiMAX DL transmission

In this section, we describe the widely used 2-D channel estimation method and the general idea of DD channel estimation method.

3.1 Two-dimensional channel estimation

In the 2-D channel estimation scheme, the CFRs of the pilots are obtained by the LS method. Then, the pilot CFRs in two adjacent even (and odd) symbols are used to estimate the CFRs of the data subcarriers with the same subcarrier indexes in the odd (respectively even) symbol in between by linear interpolation in the time domain, as shown in Figure 4. We will refer to these data subcarriers as pseudo-pilots. Next, the CFRs of other data subcarriers are obtained by linear interpolation based on CFRs of the nearest pilots and/or pseudo-pilots in the same symbol. In the following discussion, we use $\hat{H}_{2D}(k,n)$ to denote the CFR estimated by the 2-D method for subcarrier k in OFDMA symbol n.

3.2 Decision-directed channel estimation

As the number of pilots in each OFDMA symbol is very limited, it is desirable to have data subcarriers to serve as additional pilots. One way to achieve this goal is through the use of DD channel estimation method [14], as depicted in Figure 5. Let $Y(k, n)$ denote the output of fast Fourier transform (FFT) in the receiver for subcarrier k in OFDMA symbol n. These outputs, after channel compensation, are channel-decoded into data bits that in turn are re-encoded to obtain estimates of the transmitted symbols $\hat{X}(k,n)$. The CFR estimate for the subcarrier can be recalculated as

$$\hat{H}_{DD}(k,n) = \frac{Y(k,n)}{\hat{X}(k,n)}, \tag{1}$$

which can be used to estimate the CFR of the next OFDMA symbol. For better results, the CFRs of the following symbols may be predicted in the time domain by a prediction filter, as suggested in [14]. In WiMAX, however, using a prediction filter may not be a good strategy. The reason is as follows: A prediction filter is usually a finite impulse response filter. Therefore, it requires a certain number of samples to fill the filter buffer before producing any useful output. In the WiMAX frames, each DL subframe (with a length of less than 48 symbols) is preceded by a UL subframe. Since no samples are available during UL subframes, the filter outputs are not valid in the first few OFDMA symbols of each DL subframe.

The DD method is a powerful method for channel estimation. However, this method may not be applicable to the WiMAX system if the DL bursts are arbitrarily allocated, such as the one given in Figure 1. Suppose that the coded bits destined for MS no. 5, called MS-5, are located in burst no. 5. In order to use the DD approach

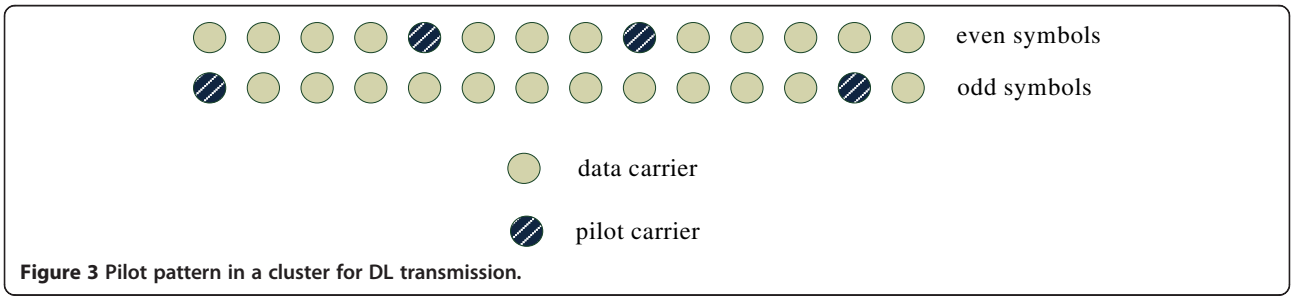

Figure 3 Pilot pattern in a cluster for DL transmission.

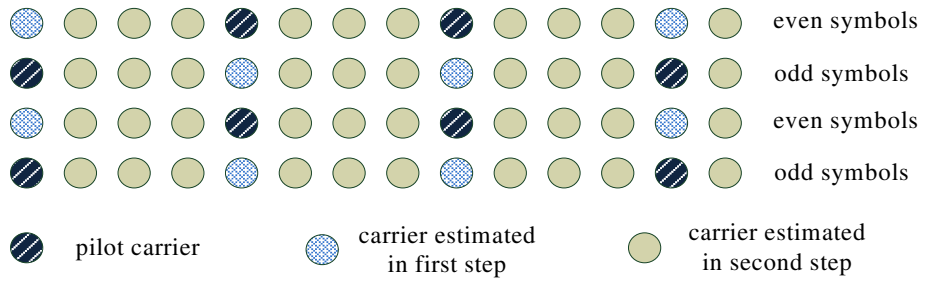

Figure 4 2-D channel estimation method.

on symbol 21, MS-5 has to (progressively) decode bursts no. 2 and no. 3 and then re-encode data bits of bursts no. 2 and no. 3. If bursts no. 2 and no. 3 are destined for MSs other than MS-5, the decoding and encoding processes of bursts no. 2 and no. 3 are the extra and unnecessary cost incurred by employing the DD method. To avoid the unnecessary cost for using the DD method, we propose a burst allocation strategy for WiMAX DL transmission.

4. Proposed burst allocation strategy and channel estimation methods

In this section, we propose a burst allocation method for WiMAX DL transmission and three DD channel estimation methods. Each DD channel estimation method can be used together with the proposed allocation method, and an MS may adopt any of the three methods depending on the allowed computational cost.

4.1 Proposed burst allocation method and application

The proposed allocation method is illustrated in Figure 6. To simplify the discussion, in Figure 6, we assume that the FCH and DL-MAP occupy all of the slots in OFDMA symbols 1 and 2. The proposed allocation method can be easily extended to the case when the assumption is not valid. Before decoding data bursts, every MS has to decode FCH and DL-MAP first. It is easy for an MS to verify the correctness of the decoded FCH and DL-MAP, as described in Section 2.1. If the FCH and DL-MAP are correctly decoded, an MS can use the DD channel estimation method by re-encoding FCH and DL-MAP to achieve better BER performance for the next two OFDMA symbols. For these DD-enabled MSs, bursts which are allocated starting from symbols 3 and 4, such as data bursts no. 1, no. 2, and no. 3 in Figure 6, have the advantage of lower error rates compared with other bursts, such as burst no. 4. Allocating bursts starting from symbols 3 and 4 is referred to as the first allocation rule. As described previously, the DD channel estimation approach can be easily applied to those slots allocated in OFDMA symbols 3 and 4. These slots are referred to as first-column slots. One way to take advantage of this improved BER performance of the slots is to allocate the hybrid automatic repeat request (HARQ) burst with as many first-column slots as possible. With lower BER in the HARQ burst, fewer retransmissions are required, and thus, higher system throughput is achieved.

Besides the first-column slots, the DD estimation method can also be used to improve the BER performance of other slots if the following allocation rule is adopted. Each coded FEC block in the bursts is assigned to consecutive slots in the same pair of OFDMA symbols, such as the blocks in symbols 3 and 4 depicted in Figure 6. This is referred to as the second allocation rule. As a coded FEC block has a size of at most six slots, the proposed block allocation is possible. If the BS fills each FEC block with a HARQ sub-burst, the receiver can employ the error detection mechanism in each sub-burst to verify the correctness of the decoded FEC blocks. Even for an FEC block without any error detection mechanism, the receiver still can use the threshold method

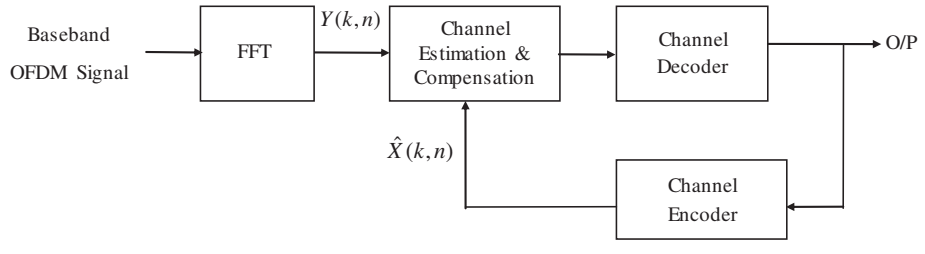

Figure 5 Concept of DD channel estimation.

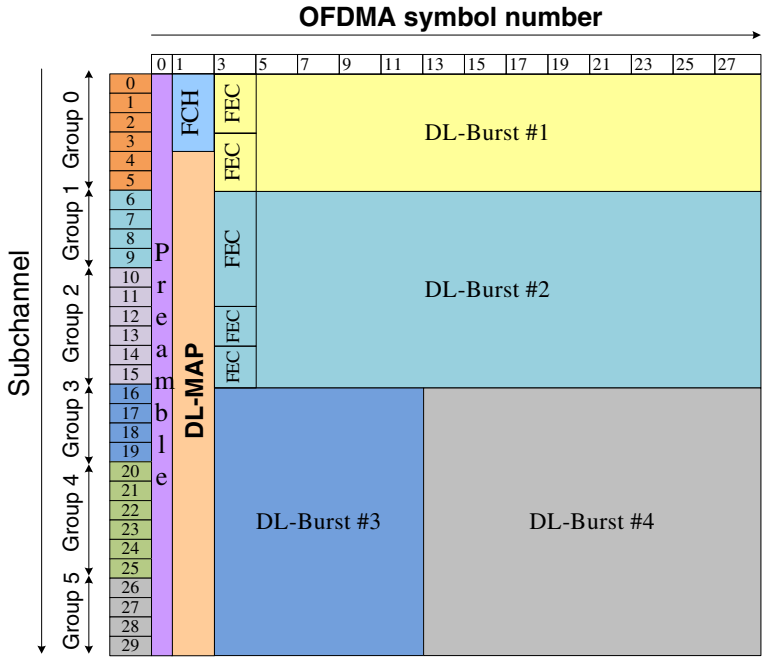

Figure 6 An example of a DL subframe and FEC blocks.

proposed in [19] to determine the correctness of the decoded block. If the FEC blocks are correctly decoded, decoded data bits can be re-encoded to enable the DD estimation method for the blocks (slots) in the next pair of OFDMA symbols. Note that if an FEC block is incorrectly decoded, the MS should not use the DD estimation scheme for blocks in the next pair of symbols. The reason is that one error data bit, after convolutional re-encoding, may incur several error coded bits, which in turn are mapped into several incorrect $\hat{X}(k,n)$ values in (1). In such a case, conventional channel estimation approach, such as the 2-D estimation method, should be adopted.

The mobile WiMAX system uses a permutation function to define the mapping between physical data subcarriers and subchannels. Since the even OFDMA symbols and the odd OFDMA symbols have different pilot patterns, subchannels may consist of different sets of physical data subcarriers in even and odd symbols. In other words, even if subchannel i in both pairs of OFDMA symbols n, $n + 1$ and $n - 2$, $n - 1$ is assigned to the same data burst, a physical subcarrier k which is assigned to subchannel i for symbols n (or $n + 1$) may not be assigned to the same subchannel for symbols $n - 1$ (respectively $n - 2$), i.e., it is not assigned to the same data burst. This fact complicates the design of the DD estimation method. Fortunately, the subchannels are divided into subchannel groups, as depicted in Figure 6, and the physical data subcarriers are permuted only within an individual subchannel group. In other words, a subchannel group consists of the same set of data and pilot subcarriers in all OFDMA symbol pairs. Thus, if all subchannels in a subchannel group are assigned to the same data burst (e.g., data bursts no. 1, no. 2, and no. 3 in Figure 6), the implementation of the DD estimation method can be simplified. This is referred to as the third allocation rule.

4.2 Time-average estimation method

A simple way for an MS to employ the DD channel estimation is to average the CFR estimates of the pair of OFDMA symbols $n - 1$ and $n - 2$ (obtained by (1)) to get CFR estimates of the next pair of symbols n and $n + 1$, i.e.,

$$\hat{H}_{\mathrm{TA}}(k,n+1) = \hat{H}_{\mathrm{TA}}(k,n) = \frac{\hat{H}(k,n-1) + \hat{H}(k,n-2)}{2}, \quad (2)$$

where $\hat{H}_{\mathrm{TA}}(k,n)$ denotes the estimated CFR of this approach which is referred to as the time-average estimation method in the following presentation. Using averaging instead of first-order extrapolation prevents the amplification of small noise which is a commonly observed phenomenon in first-order extrapolation.

4.3 Static weighted-average method

One shortcoming of the time-average estimation method is that it does not make use of the pilots in the estimated symbol pair. Thus, another possible estimation approach is to calculate CFR estimates as the weighted average of

2-D estimates $\hat{H}_{2D}(k,n)$ and time-average estimates $\hat{H}_{TA}(k,n)$. In this approach, since no *a priori* knowledge of the channel is available to the receiver, we may set the weights to be inversely proportional to the distances between the estimated data subcarrier and its neighboring reference subcarriers. For simplicity, let both the distance between two consecutive physical subcarriers and the distance between two consecutive OFDMA symbols be 1. For subcarrier k in OFDMA symbol n, let $a(k)$ be the minimum (frequency) distance between this subcarrier and a pilot/pseudo-pilot subcarrier in the same OFDMA symbol. Similarly, let $b(n)$ be the symbol distance between the current symbol (i.e., n or $n+1$ in (2)) and its closest reference symbol (i.e., $n-1$ in (2)). The weighted-average CFR estimates of subcarrier k in OFDMA symbol n is defined as

$$\hat{H}_{SW}(k,n) = \frac{b(n)}{a(k)+b(n)}\hat{H}_{2D}(k,n) + \frac{a(k)}{a(k)+b(n)}\hat{H}_{TA}(k,n). \tag{3}$$

For example, consider the subcarrier represented by the dot with red horizontal stripes in Figure 7. For this subcarrier, $a(k) = 2$ and $b(n) = 2$. Therefore, the weighted-average CFR estimate is given by $\hat{H}_{SW}(k,n) = \frac{1}{2}\hat{H}_{2D}(k,n) + \frac{1}{2}\hat{H}_{TA}(k,n)$. This estimation method is referred to as the static weighted-average method in the rest of the paper.

4.4 Adaptive weighted-average method

In the static weighted-average method, we use the same weight for the distances between physical subcarriers and between OFDMA symbols. However, these two distances may be assigned with different weights to reflect the effects of vehicle speed and channel characteristics. Since it is difficult for the receiver to pre-determine the optimal weights in (3), we propose an adaptive weighted-average method in which the weights are adaptively adjusted based on the maximum log-likelihood metric obtained in the TBCC decoding process. This method is described as follows:

Step 1. Set $u = 1$, $v = 1$ and choose a step-size constant δ with $0 < \delta < 1$.

Step 2. Calculate CFRs of all subcarriers belonging to the FEC block using

$$\hat{H}_u(k,n) = \frac{b(n)u}{a(k)+b(n)}\hat{H}_{2D}(k,n) + \left(1-\frac{b(n)u}{a(k)+b(n)}\right)\hat{H}_{TA}(k,n), \tag{4}$$

where $a(k)$ and $b(n)$ are the same as in (3). The TBCC decoder decodes the block using the estimates $\hat{H}_u(k,n)$ and saves the decoded data sequence and the corresponding log-likelihood metric.

Step 3. Similar to step 2, calculate the CFRs using

$$\hat{H}_v(k,n) = \left(1-\frac{a(k)v}{a(k)+b(n)}\right)\hat{H}_{2D}(k,n) + \frac{a(k)v}{a(k)+b(n)}\hat{H}_{TA}(k,n). \tag{5}$$

The TBCC decoder decodes the block using the estimates $\hat{H}_v(k,n)$ and saves the decoded data sequence and the corresponding log-likelihood metric.

Step 4. Set $u = u - \delta$ and $v = v - \delta$.
Step 5. Repeat steps 2 to 4 until $u < 0$and $v < 0$.
Step 6. The receiver compares the saved log-likelihood metrics and adopts the decoded data sequence with the largest metric.

Note that the adaptive weighted-average estimation method is an FEC block-based method. Thus, an MS can employ this DD estimation method only if the BS follows all three allocation rules in allocating data burst destined for the MS. One feature of this method is that it iteratively executes CFR estimation and TBCC decoding. Though FEC blocks are decoded iteratively, the computational complexity of this algorithm is not excessively high. It is due to the short codeword (with less than 288 data bits) used in each block. If necessary, the complexity can be reduced by increasing the step size δ. Moreover, when we observe the plot of log-likelihood metrics corresponding to u from 0 to 1 (and v from 1 to 0), the curve is typically similar to a downward

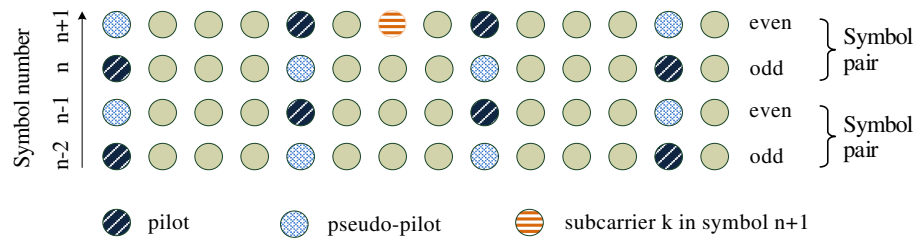

Figure 7 An example for weighted-average estimation.

parabolic curve. Therefore, a more efficient search algorithm may be developed by taking this observation into account. Finally, to further reduce the complexity, we observe that the receiver does not need to execute the search algorithm for each block. As the channel characteristics (e.g., delay spread and speed) usually do not change significantly over a short period of time, the algorithm may be executed only at the beginning of each DL frame, and the value of u (or v) thus obtained is then used throughout the subframe.

5. Theoretical analysis and simulation results

This section intends to provide both analytic evaluation and simulation results for the BER performance of the proposed estimation methods. A WiMAX DL system with parameters listed in Table 1 is used to evaluate the performances. The channel models considered are channel A and channel B of the ITU-R channel model for vehicular environments with high antenna [20] with parameters listed in Table 2, which are abbreviated as 3GVA and 3GVB in the rest of the paper, respectively.

5.1 Analytic evaluation of the bit error performance

This subsection intends to provide justification for the proposed weighted-average estimation methods based on the analytic evaluation of the BER performance of quadrature phase-shift keying (QPSK). Note that in this subsection, as no FEC is considered, the E_b/N_0 does not take into account the code rate. Suppose that the symbol transmitted in the kth subcarrier of the nth symbol is $x[k,n] = x_{k,n,i} \in \left\{ \frac{1}{\sqrt{2}}(\pm 1 \pm j) \right\}$. The received signal is given by

$$Y(k,n) = H(k,n) \cdot x_{k,n,i} + W(k,n), \tag{6}$$

where $H(k,n)$ is the CFR of subcarrier k, and $W(k,n)$ is the additive white Gaussian noise. The average BER of QPSK is equal to the pairwise symbol error rate between $x_{k,n,i} = \frac{1}{\sqrt{2}}(1+j)$ and $x_{k,n,m} = \frac{1}{\sqrt{2}}(-1+j)$. By following an argument similar to the one in [13], we find that the BER of QPSK is given by

Table 1 Parameters used in the simulation

Parameter	Value
FFT size	1,024
Number of data subcarriers per symbol	720
Number of pilot subcarriers per symbol	120
Cyclic prefix	1/8
Modulation	16 QAM
RF frequency	2.5 GHz

Table 2 Delay profiles of the channel A and B of ITU-R M.1225 [20]

Tap	Channel A		Channel B		Doppler spectrum
	Relative delay (ns)	Average power (dB)	Relative delay (ns)	Average power (dB)	
1	0	0.0	0	−2.5	Classic
2	310	−1.0	300	0.0	Classic
3	710	−9.0	8,900	−12.8	Classic
4	1,090	−10.0	12,900	−10.0	Classic
5	1,730	−15.0	17,100	−25.2	Classic
6	2,510	−20.0	20,000	−16.0	Classic

$$Q_1(a,b) - \frac{\nu_2/\nu_1}{1+\nu_2/\nu_1} I_0(ab) \exp\left[\left(-\frac{1}{2}(a^2+b^2) \right) \right]. \tag{7}$$

the variables in (7) are given as follows:
$I_m(\bullet)$ is the mth-order modified Bessel function of the first kind,

$$Q_1(a,b) = \exp\left[\left(-\frac{1}{2}(a^2+b^2) \right) \right] \cdot \sum_{m=0}^{\infty} (a/b)^m I_m(ab),$$

$$a = \left[\frac{2\nu_1^2 \nu_2 (\beta_1 \nu_2 - \beta_2)}{(\nu_1+\nu_2)^2} \right]^{1/2},$$

$$b = \left[\frac{2\nu_1 \nu_2^2 (\beta_1 \nu_1 + \beta_2)}{(\nu_1+\nu_2)^2} \right]^{1/2},$$

$$\beta_1 = 2|C|^2 \left(|\bar{X}|^2 \mu_{YY} + |\bar{Y}|^2 \mu_{XX} - \bar{X}^* \bar{Y} \mu_{XY} - \bar{X} \bar{Y}^* \mu_{XY}^* \right),$$

$$\beta_2 = C \bar{X}^* \bar{Y} + C^* \bar{X} \bar{Y}^*,$$

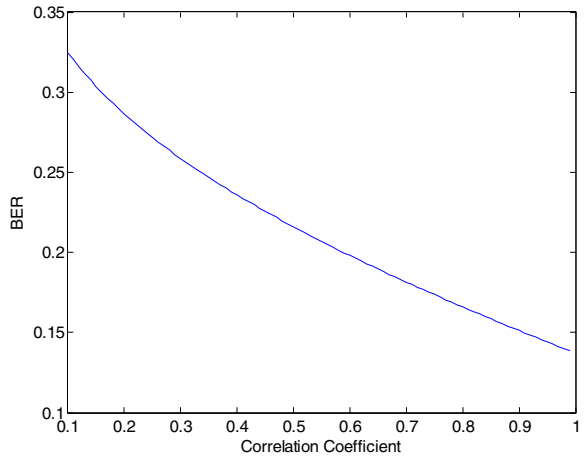

Figure 8 BER of QPSK versus correlation coefficient.

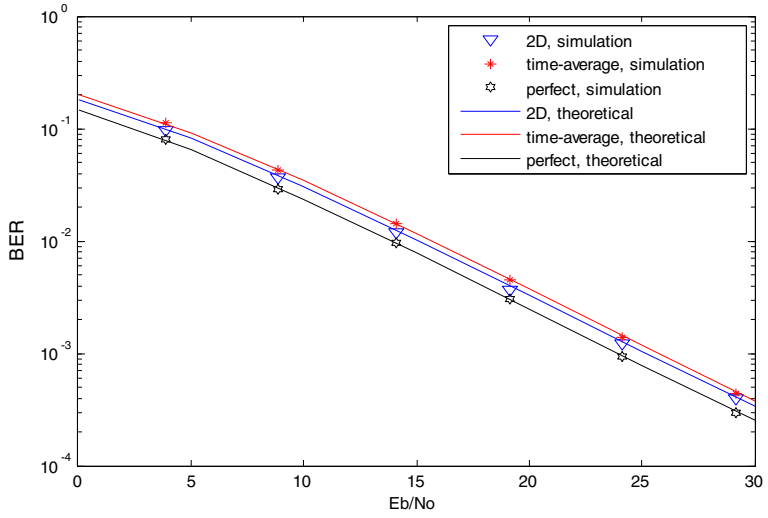

Figure 9 BERs for QPSK: Theoretical and simulation results.

$$v_1 = \sqrt{w^2 + \frac{1}{4|C^2|(\mu_{XX}\mu_{YY} - |\mu_{XY}|^2)}} - w,$$

$$v_2 = \sqrt{w^2 + \frac{1}{4|C^2|(\mu_{XX}\mu_{YY} - |\mu_{XY}|^2)}} + w,$$

$$w = \frac{C\mu_{XY}^* + C^*\mu_{XY}}{4|C|^2(\mu_{XX}\mu_{YY} - |\mu_{XY}|^2)},$$

$$C = x_{k,n,i} - x_{k,n,m} = \sqrt{2},$$

$$\bar{X} = E[X],$$

$$\bar{Y} = E[Y],$$

$$\mu_{XX} = \frac{1}{2}E\left[(X-\bar{X})(X-\bar{X})^*\right],$$

$$\mu_{YY} = \frac{1}{2}E\left[(Y-\bar{Y})(Y-\bar{Y})^*\right],$$

$$\mu_{XY} = \frac{1}{2}E\left[(X-\bar{X})(Y-\bar{Y})^*\right],$$

$$X = \hat{H}(k,n),$$

$$Y = Y(k,n).$$

The symbol '*' in the above equations denotes complex conjugation. One important property of (7) is that the average BER is inversely related to the correlation coefficient $\rho_{XY} = \frac{|\mu_{XY}|}{\sqrt{\mu_{XX}}\cdot\sqrt{\mu_{YY}}}$, as shown in Figure 8. Therefore, if we want to minimize the average BER, we need to simultaneously maximize $|\mu_{XY}|$ and minimize μ_{XX} and μ_{YY}.

We analytically evaluate μ_{XX}, μ_{YY}, and μ_{XY} in the following. It is known that the CFR of the simulated channels is given as [13]

$$H(t,f) = \sum_i \gamma_i(t)\exp[-j2\pi f\tau_i], \tag{8}$$

where $\gamma_i(t)$ and τ_i are the complex Gaussian distributed fading factor and delay time for path i, respectively. In the following discussion, we assume that $\gamma_i(t)$ remains unchanged within each OFDMA symbol, and there is no inter-subcarrier interference. As the channels considered have the property of wide-sense stationary uncorrelated scattering, the correlation between CFRs of subcarriers k_1 and k_2 in the same symbol may be computed as

$$E[H(k_1)\cdot H^*(k_2)] = \sum_i \sigma_i^2 \exp[-j2\pi\tau_i(k_1-k_2)\Delta f], \tag{9}$$

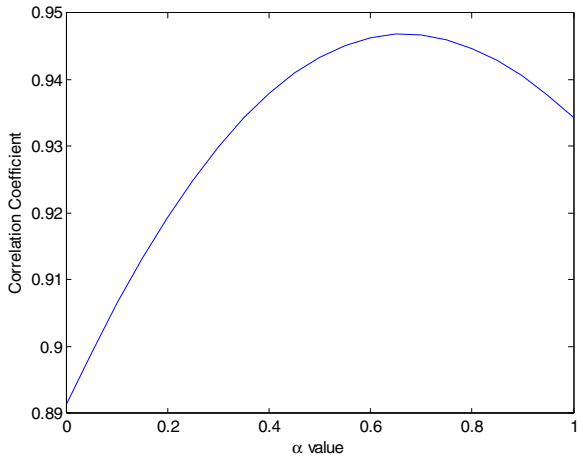

Figure 10 The correlation coefficient for different *α*.

where $\sigma_i^2 = E\left[\gamma_i(t)\gamma_i^*(t)\right]$, and Δf is the subcarrier spacing. Moreover, $\bar{X} = 0$ and $\bar{Y} = 0$, as $E[\gamma_{i(t)}] = 0$ for the considered channels. It follows that μ_{YY} is given by

$$\mu_{YY} = \frac{1}{2}\left(P_0 \cdot \left|x_{k,n,i}\right|^2 + \sigma_W^2\right), \tag{10}$$

where $P_0 = \sum_i \sigma_i^2$ is the received power, and σ_W^2 is the variance of the noise. Note that the expression for μ_{YY} is independent of channel estimation methods. Thus, if we want to decrease BER, we have to choose a channel estimation method that simultaneously maximizes $|\mu_{XY}|$ and minimizes μ_{XX}.

We now consider μ_{XY} and μ_{XX} which depend on channel estimation methods. Since μ_{XY} and μ_{XX} differ from subcarrier to subcarrier and from symbol to symbol, we will only show the equations of μ_{XY} and μ_{XX} for the specific data subcarrier represented by the dot with red horizontal stripes in Figure 7. The equations of μ_{XY} and μ_{XX} for other data subcarriers can be derived similarly.

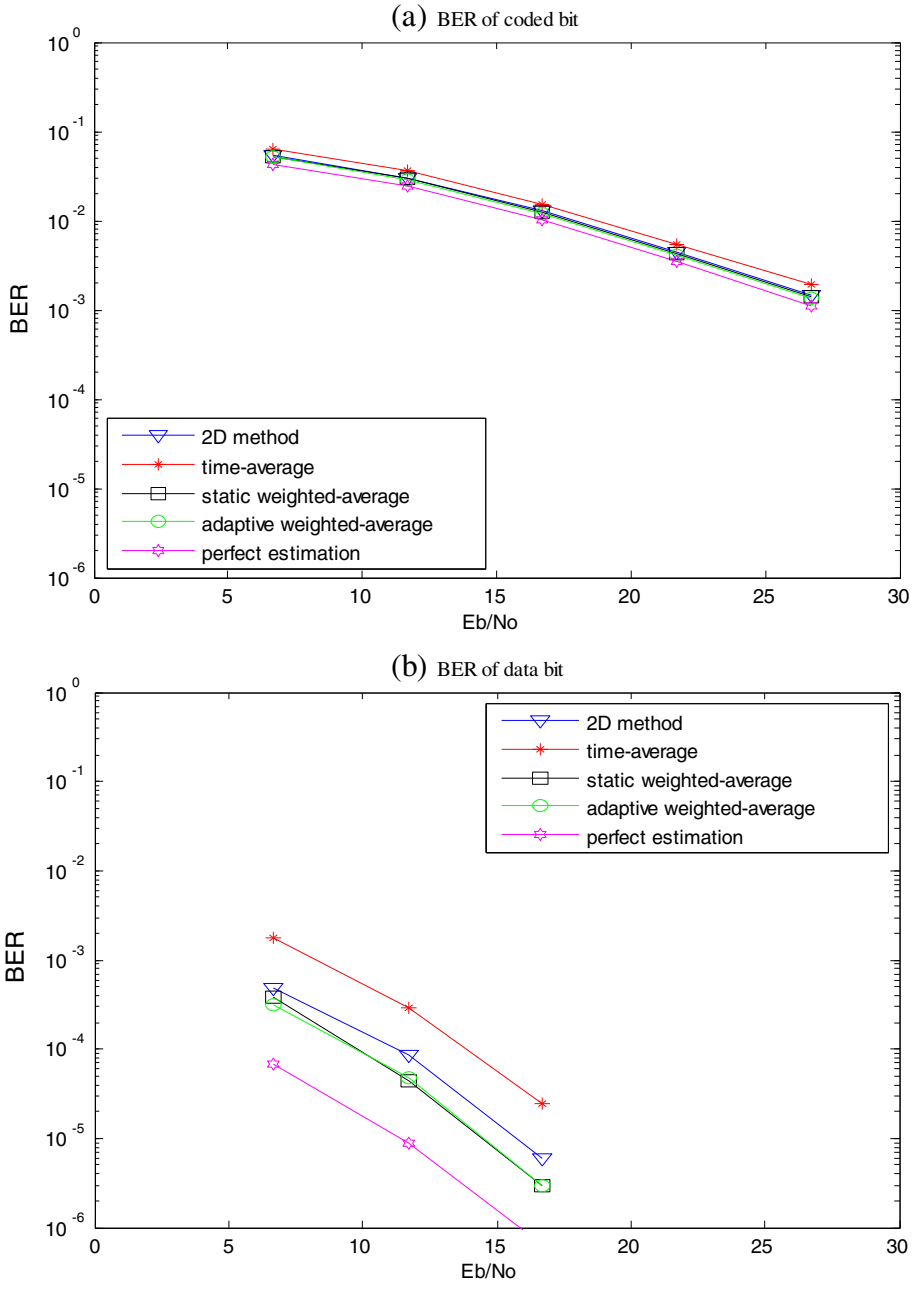

Figure 11 BER of QPSK for 3GVA with a speed of 10 km/h. (**a**) BER of coded bit. (**b**) BER of data bit.

We first consider the time-average estimation method. For the specific data subcarrier, the CFR estimate is given by

$$\hat{H}_{\mathrm{TA}}(k,n+1)=\frac{\hat{H}(k,n-1)+\hat{H}(k,n-2)}{2}. \tag{11}$$

With straightforward derivation, we find that μ_{XX} and μ_{XY} for the time-average estimation method are given by

$$\mu_{XX,\mathrm{TA}}=\frac{1}{2}\left\{P_0\left[\frac{1}{2}+\frac{1}{2}J_0(\theta_d)\right]+\frac{1}{2}\sigma_W^2\right\} \tag{12}$$

and

$$\mu_{XY,\mathrm{TA}}=\frac{1}{2}x_{k,n,i}^{*}\cdot P_0\left\{\frac{1}{2}J_0(2\theta_d)+\frac{1}{2}J_0(3\theta_d)\right\}, \tag{13}$$

respectively, where $J_0(x)$ is the zeroth-order Bessel function of the first kind, $\theta_d=2\pi T_S f_d$, T_S is the OFDMA

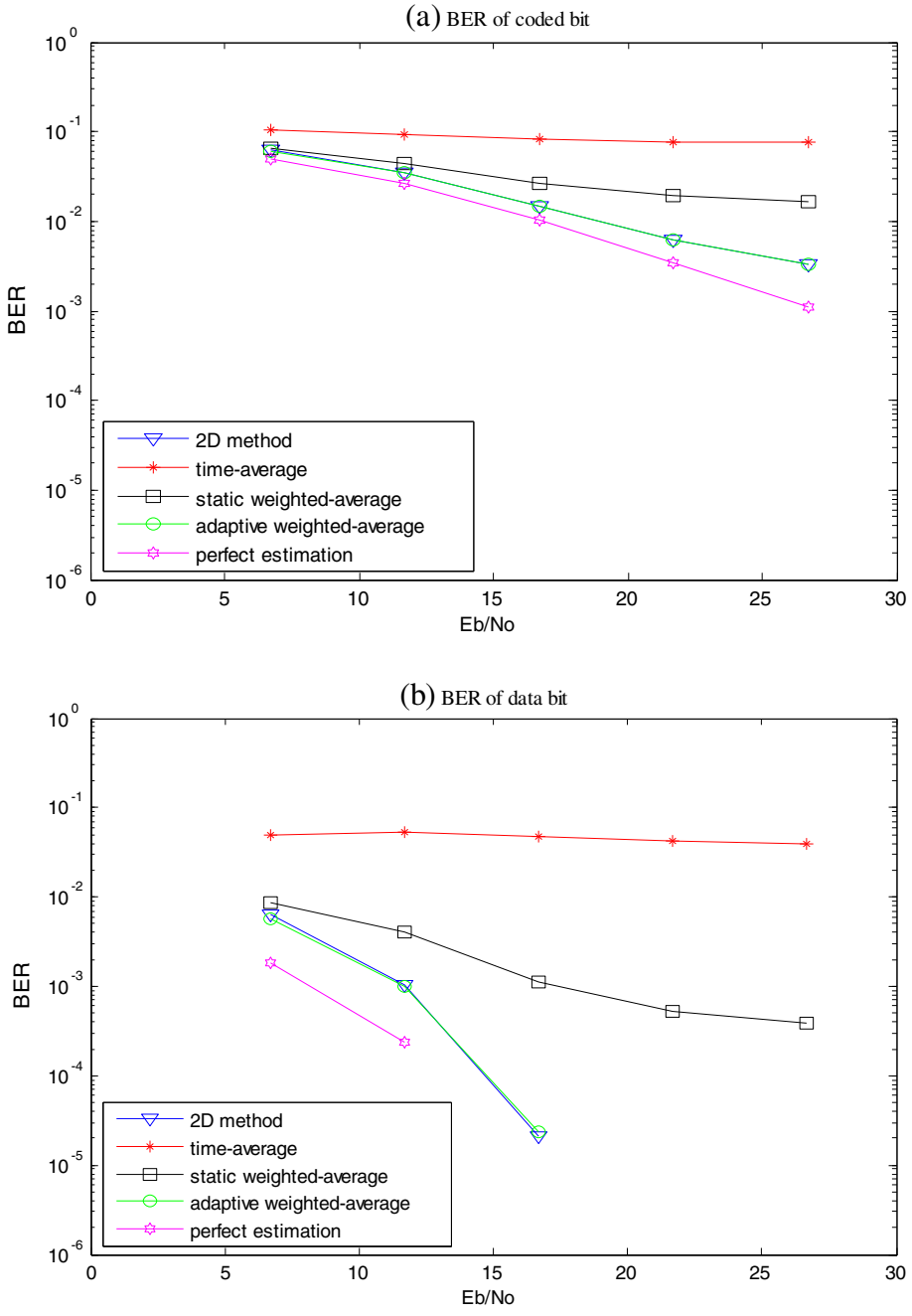

Figure 12 BER of QPSK for 3GVA with a speed of 200 km/h. (**a**) BER of coded bit. (**b**) BER of data bit.

symbol duration (including cyclic prefix), and f_d is the maximum Doppler frequency. Next, we consider the 2-D channel estimation method. For the data subcarrier in Figure 7, the CFR estimate is given by

$$\hat{H}_{2D}(k,n+1)=\frac{\hat{H}(k-2,n+1)+\hat{H}(k+2,n+1)}{2}. \tag{14}$$

A similar derivation yields the formulas for μ_{XX} and μ_{XY} of this 2-D estimate which are

$$\mu_{XX,2D}=\frac{1}{2}\left\{\frac{1}{2}P_0+\frac{1}{2}\sum_i\sigma_i^2\cos(8\pi\tau_i\Delta f)+\frac{9}{32}\sigma_W^2\right\} \tag{15}$$

and

$$\mu_{XY,2D}=\frac{1}{2}x_{k,n,i}^{*}\sum_i\sigma_i^2\cos(4\pi\tau_i\Delta f), \tag{16}$$

respectively. By substituting μ_{XX}, μ_{YY}, and μ_{XY} into (7) and averaging the BERs of all data subcarriers, we obtain the

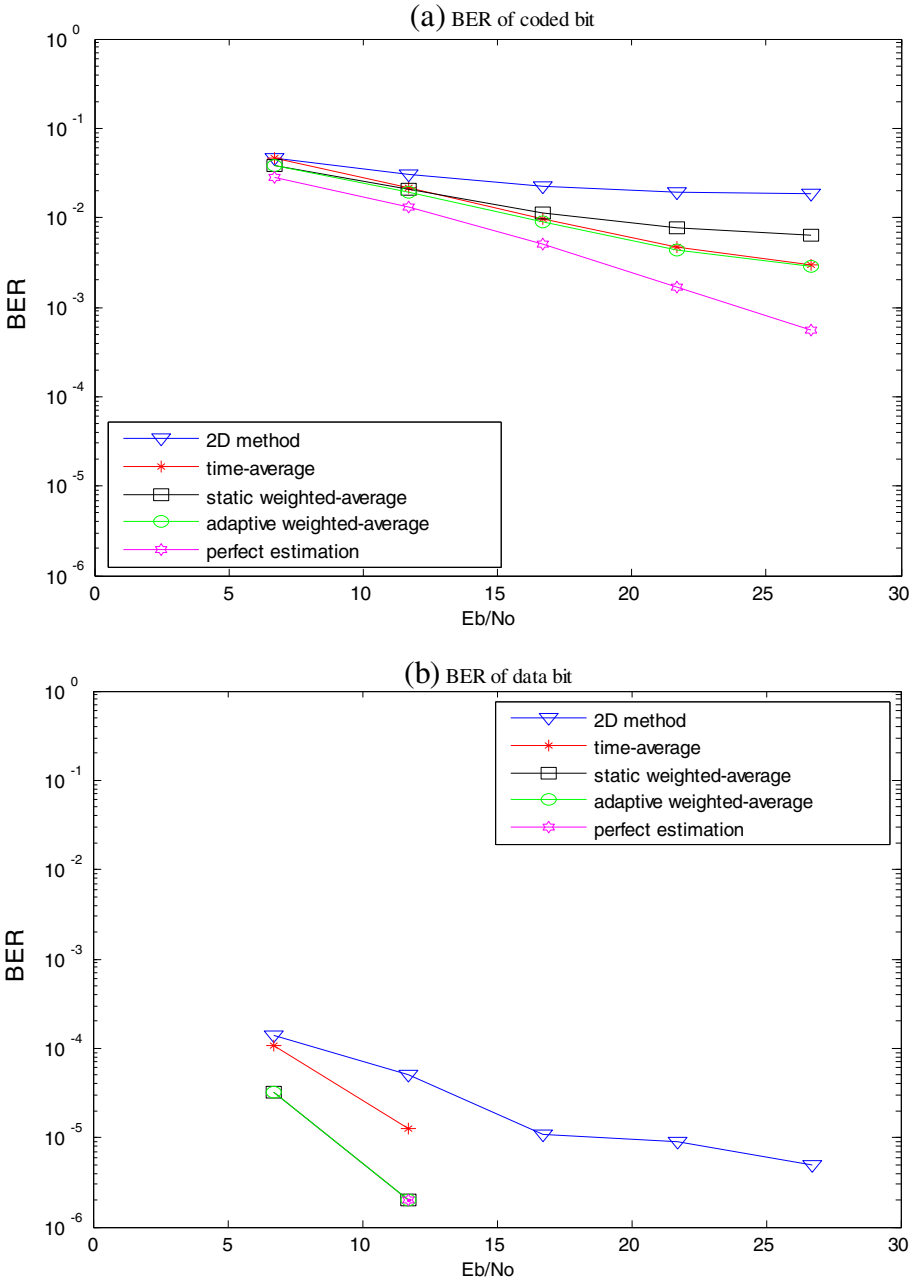

Figure 13 BER of QPSK for 3GVB with a speed of 10 km/h. (**a**) BER of coded bit. (**b**) BER of data bit.

analytic BERs of the time-average estimation method and the 2-D estimation method. Figure 9 compares the analytic BER and the BER obtained using the Monte Carlo simulation method for the time-average estimation method, 2-D estimation method, and perfect estimation (in which the receiver has perfect knowledge of the CFR) for QPSK over the 3GVA channel with speeds of 1 km/h. We find that the simulation results are very close to the analytic values.

Recall that if we want to minimize BER, we need to simultaneously maximize $|\mu_{XY}|$ and minimize μ_{XX}. Examining (12), (13), (15), and (16), we observe that there is no free variable to achieve the goal. Therefore, we introduce a new variable α, and let the CFR be estimated by

$$\hat{H}_W(k,n+1) = \alpha \cdot \frac{\hat{H}(k,n-1) + \hat{H}(k,n-2)}{2} \tag{17}$$

$$+ (1-\alpha) \cdot \frac{\hat{H}(k-2,n+1) + \hat{H}(k+2,n+1)}{2},$$

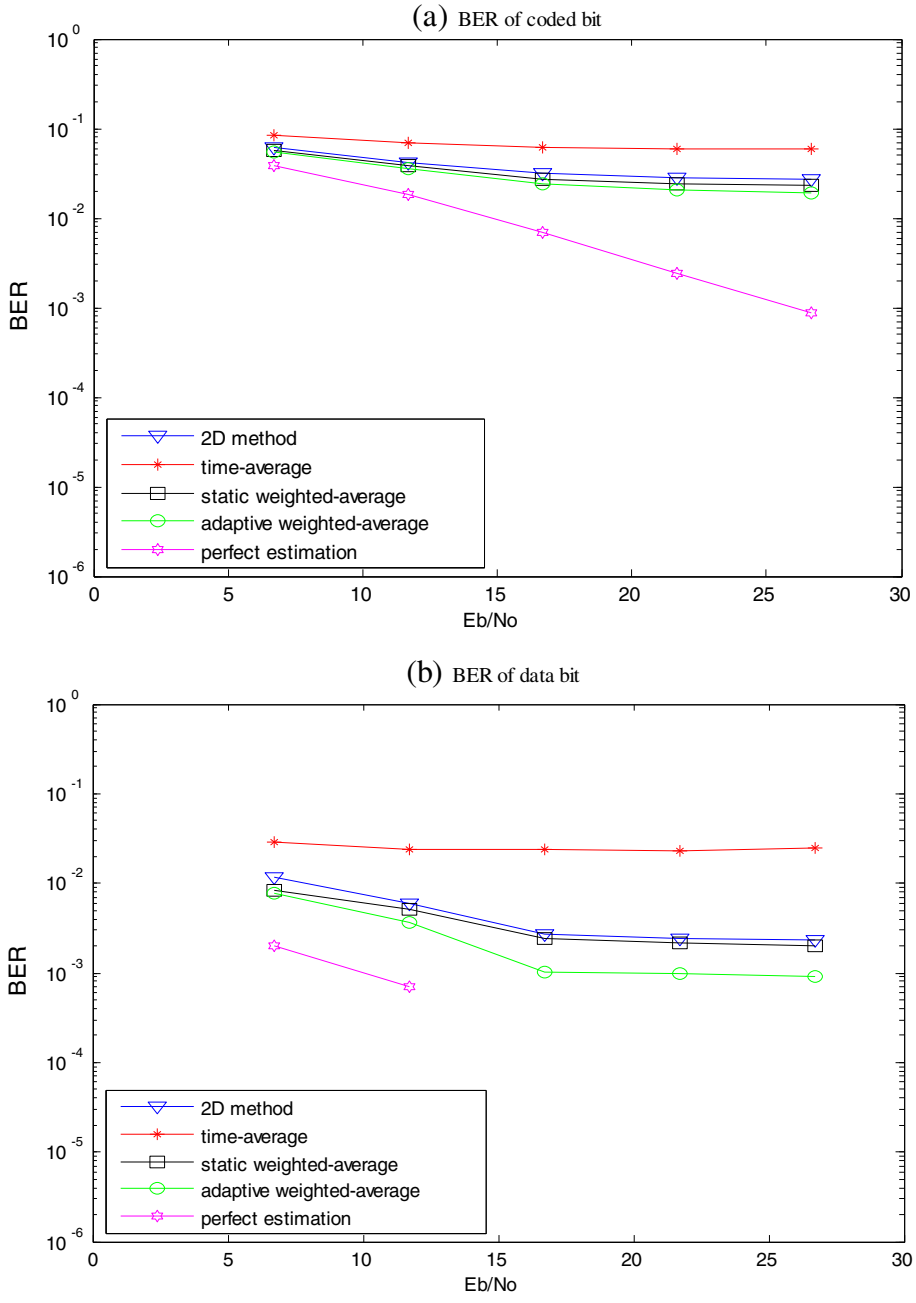

Figure 14 BER of QPSK for 3GVB with a speed of 200 km/h. (**a**) BER of coded bit. (**b**) BER of data bit.

Which is a weighted average of the time-average estimate and 2-D estimate. The expressions of μ_{XX} and μ_{XY} of this estimation method are given by

$$\begin{aligned}\mu_{XX,W} &= \frac{1}{2}\alpha^2\left\{P_0\left(\frac{1}{2}+\frac{1}{2}J_0(\theta_d)\right)+\frac{1}{2}\sigma_W^2\right\}\\ &+\frac{1}{2}(1-\alpha^2)\left\{\frac{1}{2}P_0+\frac{1}{2}\sum_i\sigma_i^2\cos(8\pi\tau_i\Delta f)+\frac{9}{32}\sigma_W^2\right\}\\ &+2\cdot\frac{\alpha(1-\alpha)}{4}\{J_0(2\theta_d)+J_0(3\theta_d)\}\cdot\left(\sum_i\sigma_i^2\cos(4\pi\tau_i\Delta f)\right)\end{aligned} \tag{18}$$

and

$$\mu_{XY,W}=\frac{1}{2}x_{k,n,i}^*\left\{\frac{\alpha}{2}P_0[J_0(2\theta_d)+J_0(3\theta_d)]+(1-\alpha)\left[\sum_i\sigma_i^2\cos(4\pi\tau_i\Delta f)\right]\right\}, \tag{19}$$

respectively. Based on (10), (18), and (19), we can compute the correlation coefficient of the weighted-average estimate for this data subcarrier. Figure 10 plots the correlation coefficient versus α for the 3GVB channel with a speed of 100

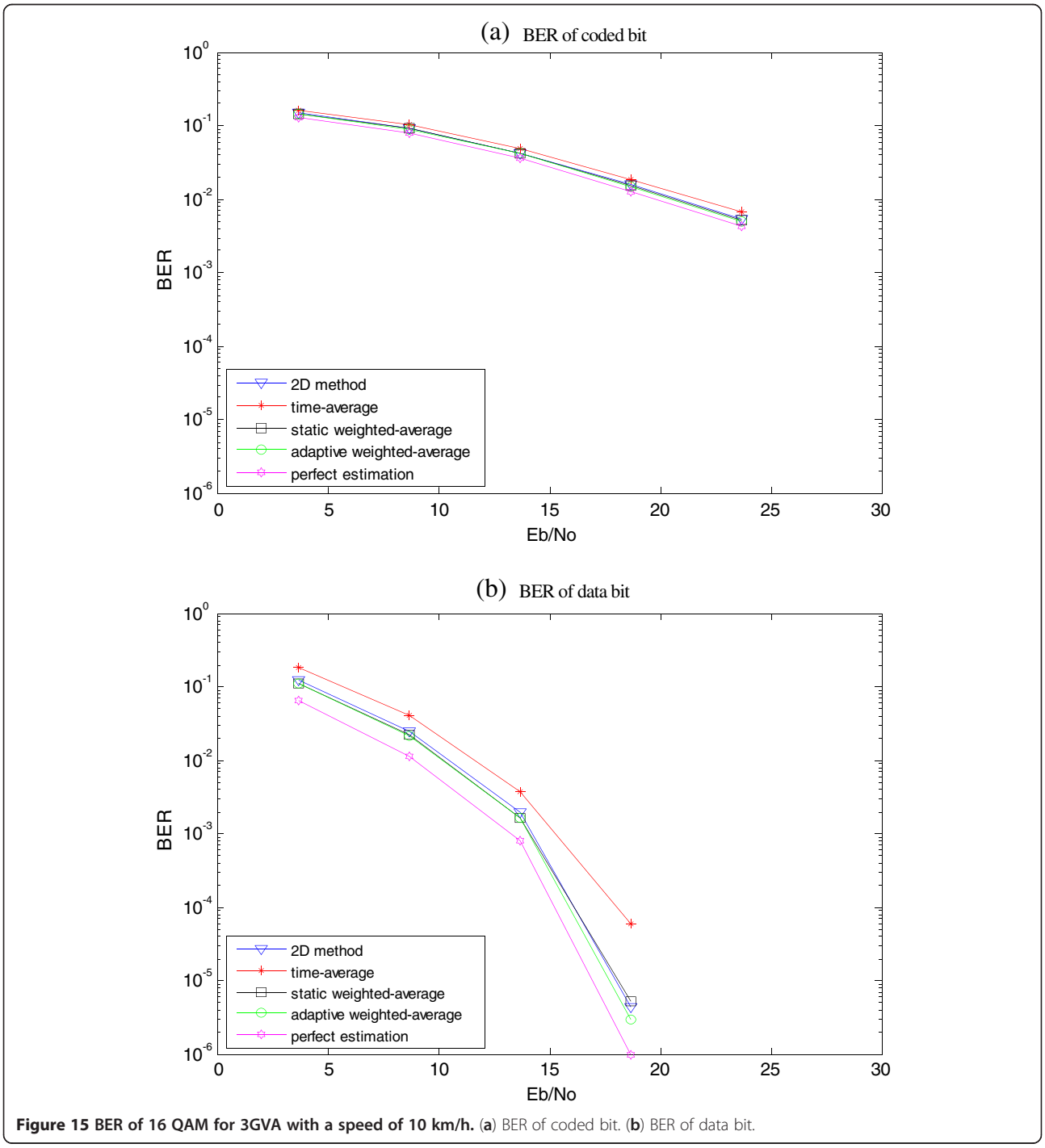

Figure 15 BER of 16 QAM for 3GVA with a speed of 10 km/h. (**a**) BER of coded bit. (**b**) BER of data bit.

km/h and E_b/N_0 = 10 dB. The figure shows that the correlation coefficient is maximized when $\alpha \approx 0.65$. Therefore, we conclude that using the weighted-average estimation method can achieve better BER performance provided that we can find a good value of α. Although we show only the formulas for one particular data subcarrier here, the general case, though much more complicated, is similar.

We now consider the implementation issue for the weighted-average estimation method. The optimal value of α depends on channel characteristics. Since no channel information is available at the receiver, it is not possible to optimize the correlation coefficient analytically. Instead, the adaptive weighted-average method is suggested in this paper to search for a good α value without channel information.

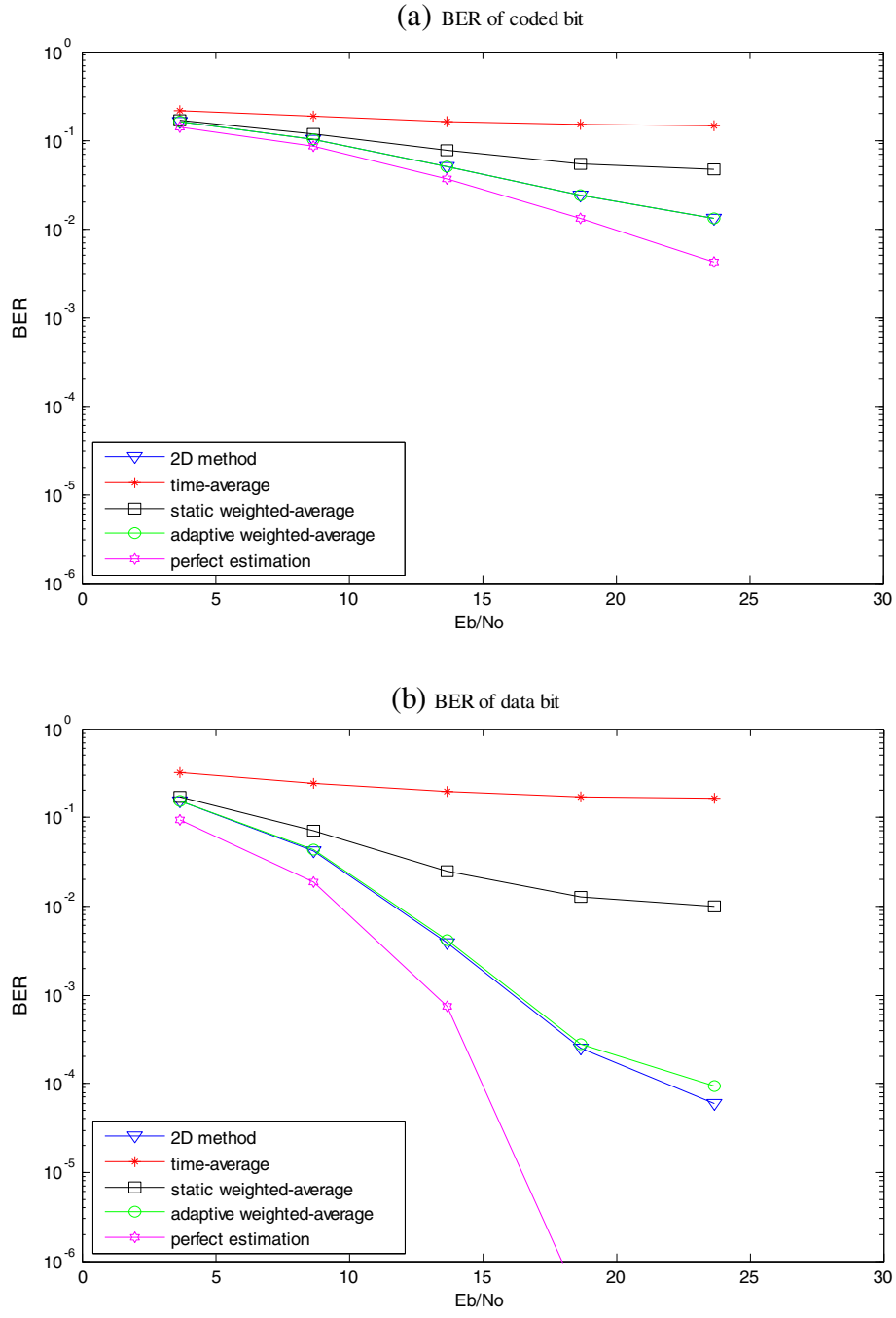

Figure 16 BER of 16 QAM for 3GVA with a speed of 200 km/h. (**a**) BER of coded bit. (**b**) BER of data bit.

5.2 Simulation results

In this subsection, we present the simulation results of the BER performances for the proposed estimation methods. The performances of the conventional 2-D method and perfect estimation are also obtained to serve as benchmarks for comparison. Since the performance of the adaptive weighted-average estimation method depends on the FEC encoding methods, we use the rate-1/2 TBCC in all the experiments in this subsection, and the code rate has been taken into account in the E_b/N_0 in all figures. Note that in the experiments, only frames with correctly decoded FCH and DL-MAP are included in the calculation of BER, as no MS can proceed to decode data bursts without correct FCH and DL-MAP information.

Figures 11, 12, 13, and 14 plot the BERs of the demodulated coded bits and decoded data bits for QPSK

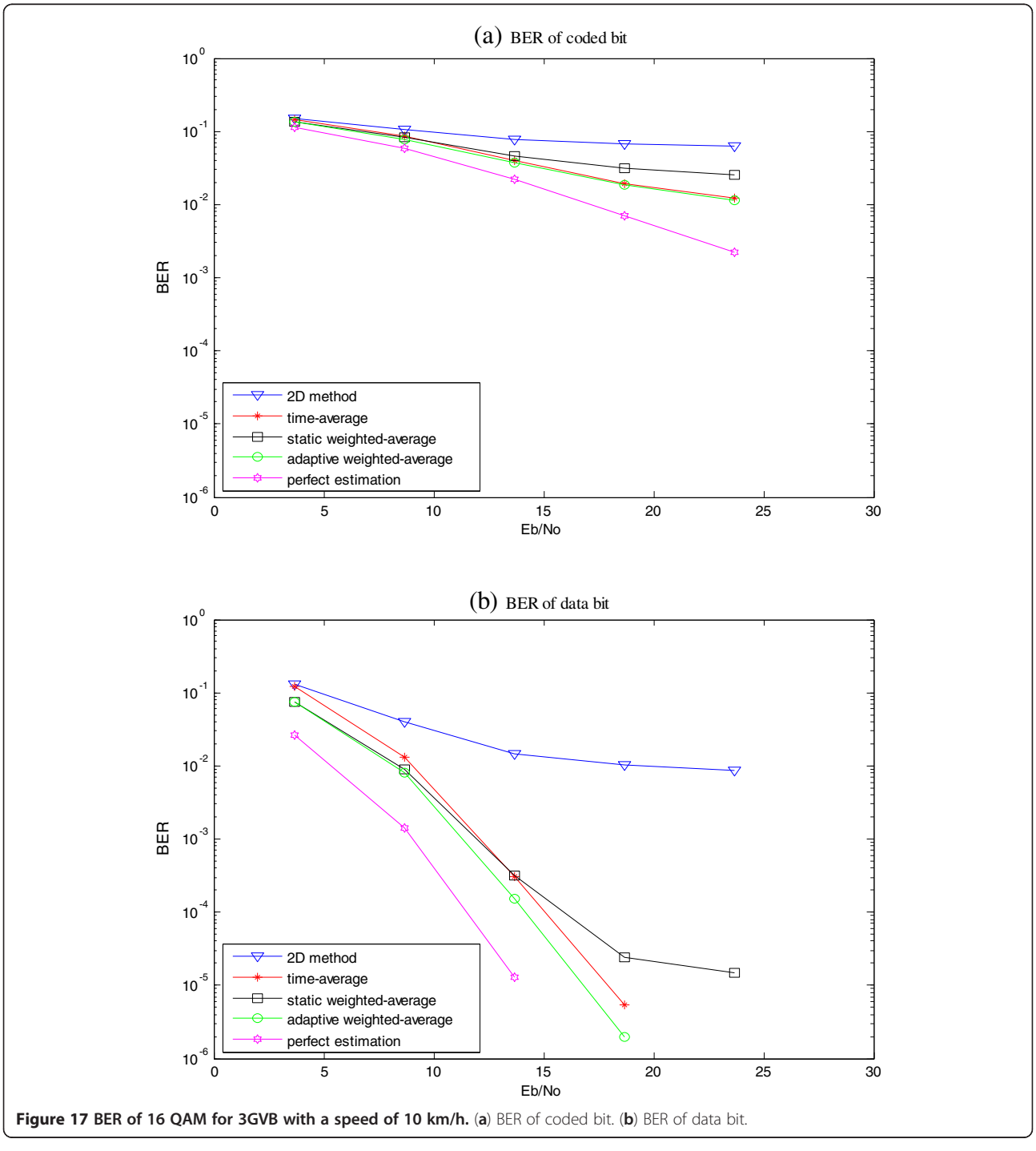

Figure 17 BER of 16 QAM for 3GVB with a speed of 10 km/h. (**a**) BER of coded bit. (**b**) BER of data bit.

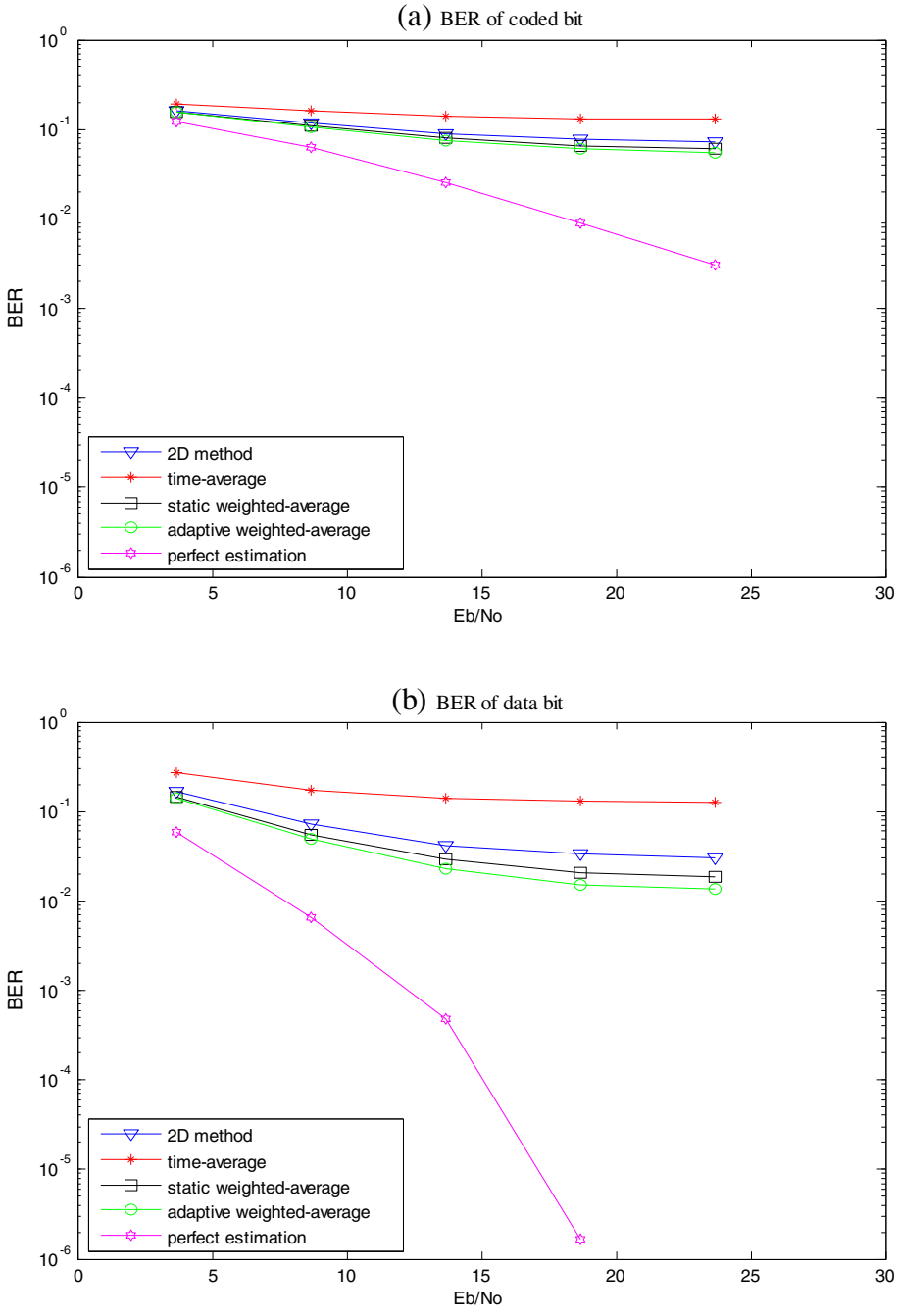

Figure 18 BER of 16 QAM for 3GVB with a speed of 200 km/h. (**a**) BER of coded bit. (**b**) BER of data bit.

over the 3GVA and 3GVB channels with two speeds, 10 and 200 km/h. For comparison, the BERs for 16 QAM and 64 QAM are plotted in Figures 15, 16, 17, and 18 and Figures 19, 20, 21, and 22 for the same channel models, respectively. Since the delay spread of the 3GVB channel is much larger than that of the 3GVA channel, accurate estimation of CFR for the 3GVB channel is generally much more difficult. From the figures, we observe that for low speed, the 2-D estimation method outperforms the proposed time-average estimation method if the channel model is 3GVA (i.e., with small delay spread) and vice versa if the channel model is 3GVB (i.e., with large delay spread). This is because for the large-delay-spread channel, the coherent bandwidth of the channel is relatively small, which drastically reduces the accuracy of subcarrier domain interpolation

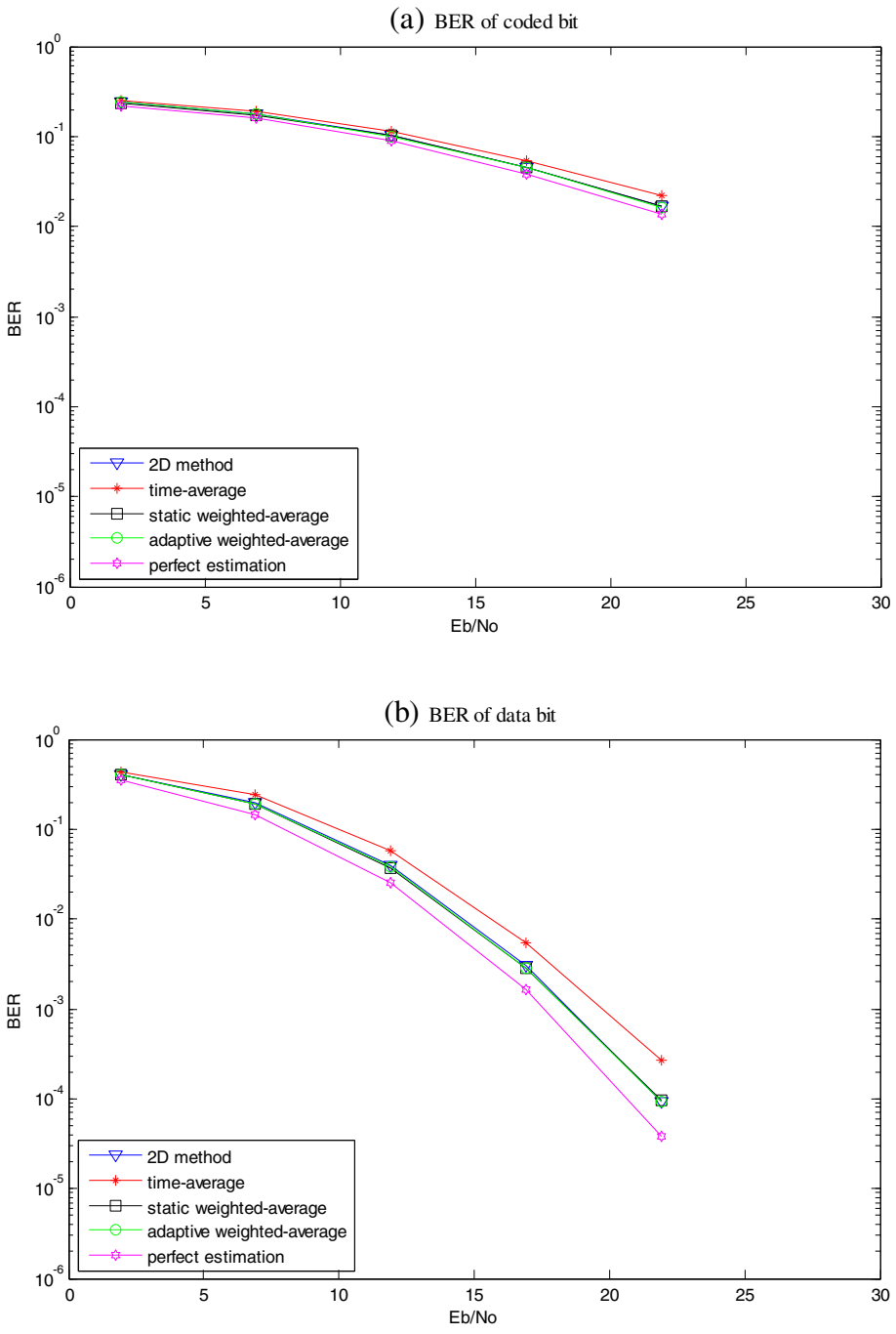

Figure 19 BER of 64 QAM for 3GVA with a speed of 10 km/h. (**a**) BER of coded bit. (**b**) BER of data bit.

(i.e., frequency domain interpolation) estimation in the 2-D method. We also observe that for channel models with high speed (200 km/h), the 2-D estimation method outperforms the proposed time-average estimation, since in the rapid changing channel it is difficult to estimate the CFR using only the time domain interpolation. The simulation results imply that using either approach alone does not yield good performance for all cases. Therefore, a better estimation approach is to introduce a new variable α and combine these two estimation methods with weights, α and $1 - \alpha$, as suggested in the theoretical analysis. The experimental results show that the static weighted-average estimation method outperforms at least one but not necessarily both of the two constituent estimation methods. For example, its performance is much worse than that of the 2-D estimation

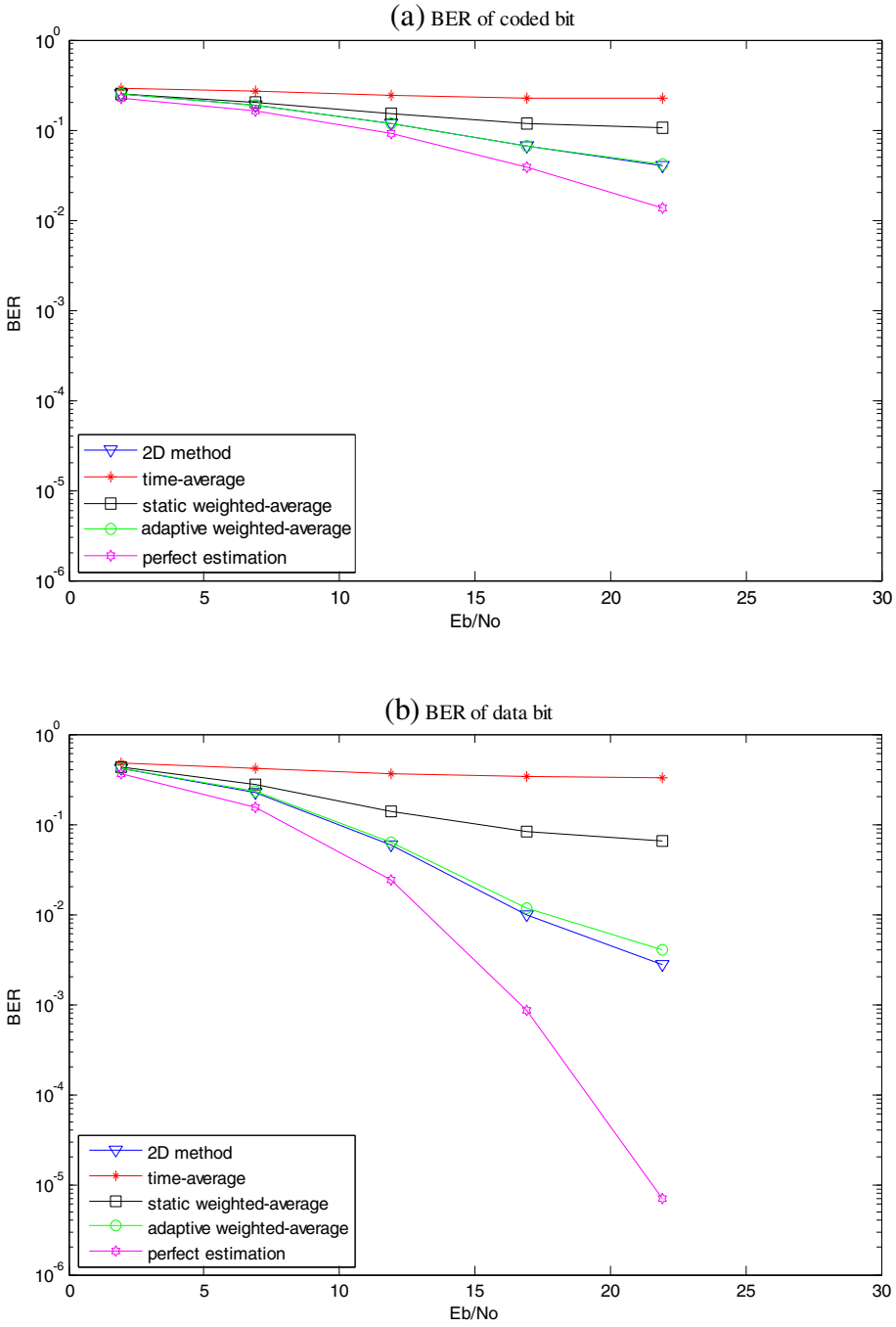

Figure 20 BER of 64 QAM for 3GVA with a speed of 200 km/h. (**a**) BER of coded bit. (**b**) BER of data bit.

method for the 3GVA channel with a speed of 200 km/h. The observation is in agreement with the theoretical analysis. Since the variable α in the static weighted-average estimation method may not be optimal, it can be observed from Figure 10 that there is no guarantee that the weighted-average estimation performs better than both the time-average estimation and 2-D estimation. The results strongly suggest that the variable α (and thus, the weights) should be adaptive in order to provide a relatively better BER performance for all types of channels. The experimental results confirm that the adaptive weighted-average estimation method indeed achieves a performance equal to or better than those attained by all other estimation methods for all considered channels.

The 3GVB channel with a speed of 200 km/h is the most difficult channel to estimate among the four channels

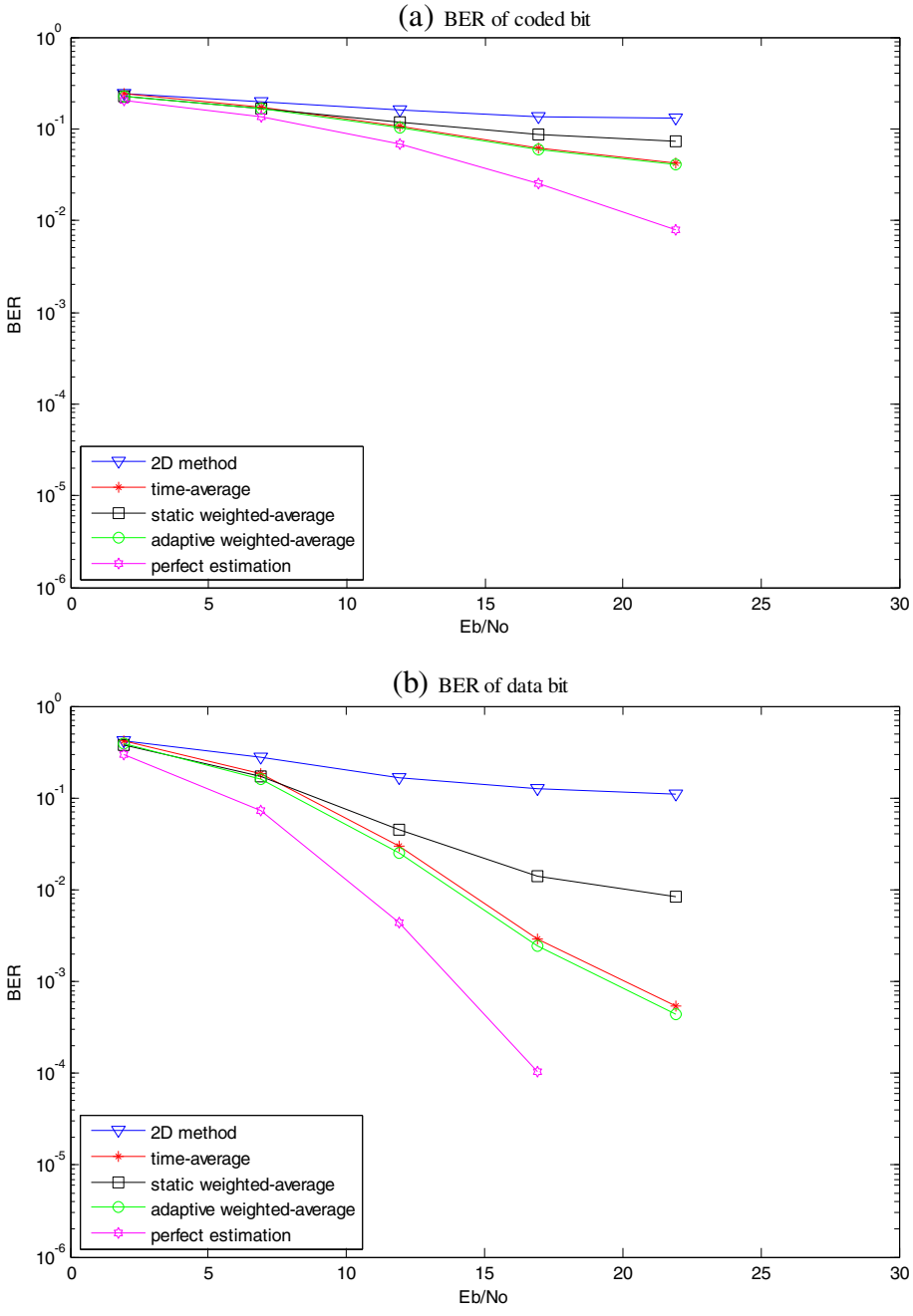

Figure 21 BER of 64 QAM for 3GVB with a speed of 10 km/h. (**a**) BER of coded bit. (**b**) BER of data bit.

considered. From Figures 14, 18, and 22, we observe that both weighted-average estimation methods outperform the 2-D estimation and time-average estimation in this case. This result is not surprising. As with larger delay spread and higher speed, the CFR fluctuates rapidly across frequency and time. Thus, additional pilots brought in by mixture strategies improve the BER performance. Incidentally, since the length of an FEC block is 288 data bits, we find that only the adaptive weighted-average estimation method with QPSK achieves an acceptable BER (approximately 10^{-3}) for $E_b/N_0 \geq 15$ dB.

6. Conclusions

It is well known that the DD channel estimation method performs well in OFDM systems. Though a derivative of the OFDM, the OFDMA used in the WiMAX DL system is different in that subcarriers are partitioned into different groups destined for different MSs. To account

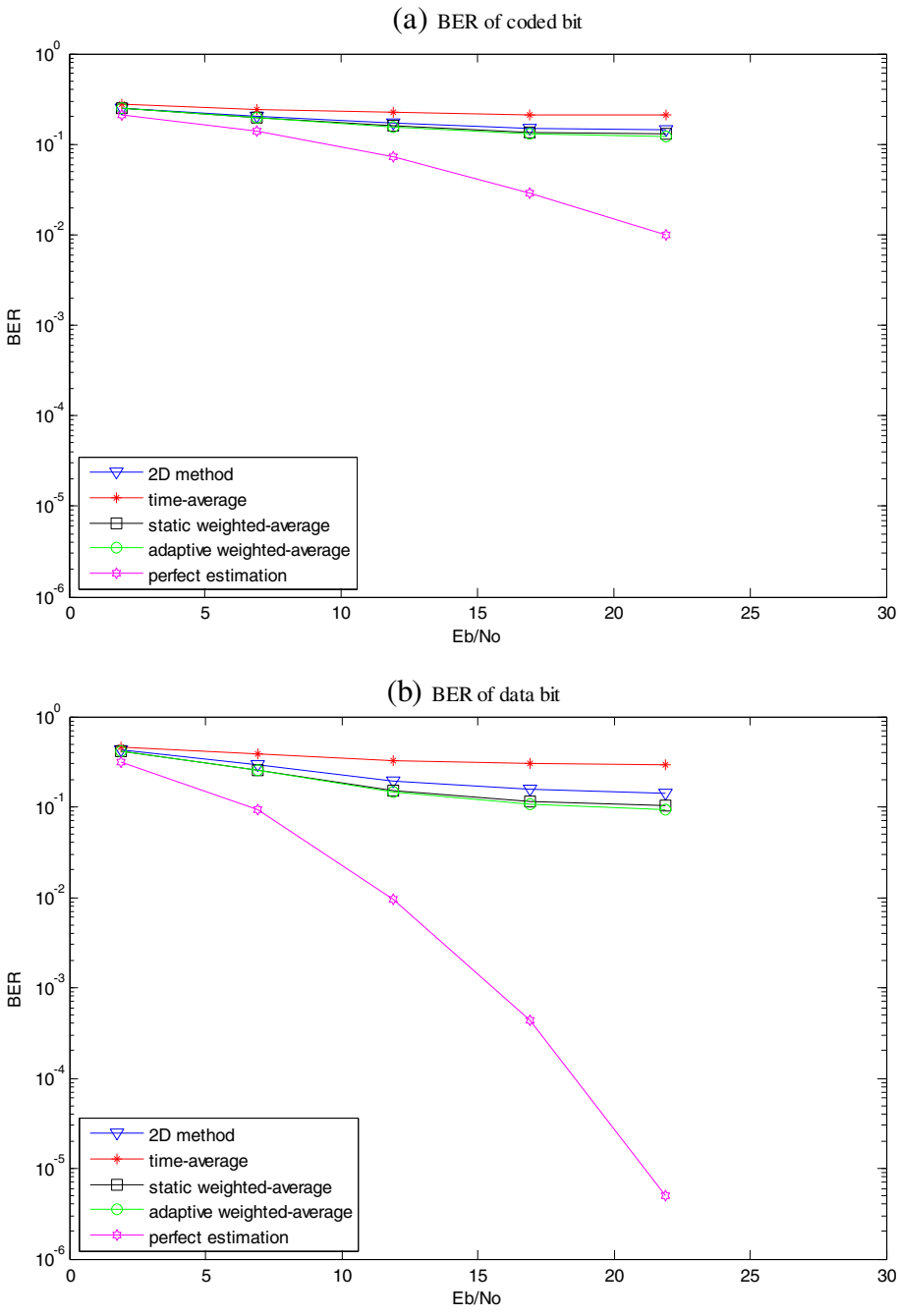

Figure 22 BER of 64 QAM for 3GVB with a speed of 200 km/h. (**a**) BER of coded bit. (**b**) BER of data bit.

for this difference, we propose an allocation method for WiMAX DL data bursts so that the destination MSs can apply DD channel estimation to these bursts without demodulating data bursts intended for other MSs. In addition, the DD channel estimation method must be adapted to account for the WiMAX frame structure. To this end, three DD channel estimation methods based on the proposed allocation method are suggested. Theoretical analysis strongly suggests that, among the three proposed estimation methods, the adaptive weighted-average estimation method may achieve the best performance. Simulation results confirm this for the four channel models considered. Moreover, in the worst case scenario where the channel suffers from a large delay spread, it is found that the proposed adaptive weighted-average estimation method significantly outperforms the widely used 2-D estimation method. For the consideration of implementation, we also discuss various ways to

reduce the complexity of the proposed adaptive algorithm. Overall, the proposed allocation method and the adaptive weighted-average estimation method can be applied to the WiMAX DL transmission to improve the BER performance for error-sensitive data, such as HARQ.

Competing interests
The authors declare that they have no competing interests.

Acknowledgments
Research support from the National Science Council, Taiwan, ROC, under grants 97-2218-E-027-010 and 97-2218-E-027-009 is gratefully acknowledged.

Author details
[1]Department of Electronic Engineering, National Taipei University of Technology, 1, Sec. 3, Chung-Hsiao E. Rd., Taipei 106, Taiwan. [2]Department of Computer Science and Information Engineering, National Taipei University of Technology, 1, Sec. 3, Chung-Hsiao E. Rd., Taipei 106, Taiwan.

Received: 13 November 2012 Accepted: 14 May 2013
Published: 4 June 2013

References
1. IEEE, *IEEE 802.16e-2005 and IEEE Std 802.16-2004/Cor 1–2005 (Amendment and Corrigendum to IEEE Std 802.16-2004), IEEE Standard for Local and Metropolitan Area Networks. Part 16: Air Interface for Fixed and Mobile Broadband Wireless Access Systems. Amendment 2: Physical and Medium Access Control Layers for Combined Fixed and Mobile Operation in Licensed Bands and Corrigendum 1, 2006* (IEEE, New York, 2006)
2. M Morelli, U Mengali, A comparison of pilot-aided channel estimation methods for OFDM system. IEEE Trans. Signal Processing **49**(12), 3065–3073 (2001)
3. X Dong, W-S Lu, ACK Soong, Linear interpolation in pilot symbol assisted channel estimation for OFDM. IEEE Trans. Wireless Commun. **6**, 1910–1920 (2007)
4. I Barhumi, G Leus, M Moonen, MMSE estimator of basis expansion models for rapidly time-varying channels, in *Proceedings of European Signal Processing Conference* (, Antalya, Turkey). 4–8 September 2005, pp. 1–5
5. MD Nisar, W Utschick, T Hindelang, Maximally robust 2-D channel estimation for OFDM systems. IEEE Trans. Signal Processing **58**(6), 3163–3172 (2010)
6. F Sanzi, J Speide, An adaptive two-dimensional channel estimator for wireless OFDM with application to mobile DVB-T. IEEE Trans. Broadcasting **46**(2), 128–133 (2000)
7. S Coleri, M Ergen, A Puri, A Bahai, 2002. Proceedings of IEEE 56th Vehicular Technology Conference **2**, 894–898 (2002)
8. T Yucek, MK Ozdemir, H Arslan, FE Retnasothie, A comparative study of initial downlink channel estimation algorithms for mobile WiMAX, in *Proceedings of IEEE Mobile WiMAX Symposium* (, Orlando, Florida). 25–29 March 2007, pp. 32–37
9. M Marey, M Guenach, H Steendam, Code-aided channel tracking and frequency offset-phase noise elimination for multicarrier systems. IEEE Signal Processing Letters **15**, 657–660 (2008)
10. GA Al-Rawi, TY Al-Naffouri, A Bahai, J Cioffi, Exploiting error-control coding and cyclic prefix in channel estimation for coded OFDM systems. IEEE Commun. Letters **7**(8), 388–390 (2003)
11. M Guenach, F Simoens, H Wymeersch, H Steendam, M Moeneclaey, Code-aided Bayesian parameter estimation for multi-carrier systems. European Trans. Telecommunications **17**(6), 639–650 (2006)
12. Y Shen, E Martinez, *Wimax channel estimation: algorithms and implementations, Freescale Semiconductor Application Note, document number: AN3429, 2007*. http://code.ucsd.edu/~yushen/publications_files/Yushi%20Shen-July07-Freescale-WiMAX.pdf. Accessed 24 May 2013
13. SD You, K-Y Chen, Y-S Liu, Cubic convolution interpolation function with variable coefficients and its application to channel estimation for IEEE 802.16 initial downlink. IET Commun. **6**, 1979–1987 (2012)
14. M Bossert, A Donder, V Zyablo, Improved channel estimation with decision feedback for OFDM systems. Electronics Letters **34**(11), 1064–1065 (1998). May
15. *WiMAX Forum, Mobile WiMAX – Part I: a technical overview and performance evaluation, 2006*. http://www.wimaxforum.org/news/downloads/Mobile_WiMAX_Part1_Overview_and_Performance.pdf. Accessed 24 May 2013
16. HH Ma, JK Wolf, On tail biting convolutional codes. IEEE Trans. Commun. **34** (2), 104–111 (1986)
17. Y-S Liu, Y-Y Tsai, Minimum decoding trellis length and truncation depth of wrap-around Viterbi algorithm for TBCC in mobile WiMAX. EURASIP J. Wireless Commun. and Networking **2011**, 111 (2011)
18. *EBU, Digital video broadcasting (DVB), framing structure, channel coding and modulation for digital terrestrial television, ETSI EN 300 744, v1.5.1, 2004*. http://www.etsi.org/deliver/etsi_en/300700_300799/300744/01.05.01_40/en_300744v010501o.pdf. Accessed 24 May 2013
19. H-T Pai, YS Han, Y-J Chu, New HARQ scheme based on decoding of tail-biting convolutional codes in IEEE 802.16e. IEEE Trans. Veh. Technol. **60**, 912–918 (2011)
20. *International Telecommunication Union, Guidelines for evaluation of radio transmission technologies for IMT-2000, Recommendation ITU-R M.1225, 1997*. http://www.itu.int/dms_pubrec/itu-r/rec/m/R-REC-M.1225-0-199702-I!!PDF-E.pdf. Accessed 24 May 2013

doi:10.1186/1687-1499-2013-153
Cite this article as: Liu *et al.*: Burst allocation method to enable decision-directed channel estimation for mobile WiMAX downlink transmission. *EURASIP Journal on Wireless Communications and Networking* 2013 **2013**:153.